Draft version May 19, 2010
Preprint typeset using LaTeX style emulateapj v. 11/10/09

SLAC-PUB-14215

LIMITING ACCRETION ONTO MASSIVE STARS BY FRAGMENTATION-INDUCED STARVATION

Thomas Peters[1,2] and Ralf S. Klessen[2,3], Mordecai-Mark Mac Low[4], Robi Banerjee[2]

Draft version May 19, 2010

ABSTRACT

Massive stars influence their surroundings through radiation, winds, and supernova explosions far out of proportion to their small numbers. However, the physical processes that initiate and govern the birth of massive stars remain poorly understood. Two widely discussed models are monolithic collapse of molecular cloud cores and competitive accretion. To learn more about massive star formation, we perform simulations of the collapse of rotating, massive, cloud cores including radiative heating by both non-ionizing and ionizing radiation using the FLASH adaptive mesh refinement code. These simulations show fragmentation from gravitational instability in the enormously dense accretion flows required to build up massive stars. Secondary stars form rapidly in these flows and accrete mass that would have otherwise been consumed by the massive star in the center, in a process that we term fragmentation-induced starvation. This explains why massive stars are usually found as members of high-order stellar systems that themselves belong to large clusters containing stars of all masses. The radiative heating does not prevent fragmentation, but does lead to a higher Jeans mass, resulting in fewer and more massive stars than would form without the heating. This mechanism reproduces the observed relation between the total stellar mass in the cluster and the mass of the largest star. It predicts strong clumping and filamentary structure in the center of collapsing cores, as has recently been observed. We speculate that a similar mechanism will act during primordial star formation.

1. INTRODUCTION

Understanding the formation of massive stars is of pivotal importance in modern astrophysics. Massive stars are rare and short lived. However, they are also very bright and allow us to reach out to the far ends of the universe. For example, the most distant galaxies in the Hubble Ultra Deep Field are all characterized by vigorous high-mass star formation. Understanding the origin of massive stars, at present and at early times, therefore is a prerequisite to understanding cosmic history. In our own Milky Way, high-mass stars contribute the bulk of the UV radiation field. This radiation can ionize hydrogen and dissolve molecules. Expanding H II regions, bubbles of ionized gas surrounding massive stars, have been identified as an important source of interstellar turbulence. The complex interplay between gas dynamics and radiation thus is a key element of the evolution of the interstellar medium (ISM) and the Galactic matter cycle. Furthermore, stars are the primary source of chemical elements heavier than the hydrogen, helium, and lithium that were produced in the Big Bang. Again, massive stars have a disproportionally large share in the enrichment history of the Galaxy and the universe as a whole. It is the violent supernova explosions associated with the death of high-mass stars that contribute most of the metals. Because they insert large amounts of energy and momentum input, supernovae at the same time strongly stir up the ISM and provide for the effective mixing of the newly bread elements.

Despite their importance, the physical processes that initiate and control the build-up of massive stars are still not well understood and subject of intense debate (Mac Low & Klessen 2004; Zinnecker & Yorke 2007; McKee & Ostriker 2007). Because their formation time is short, of order of 10^5 yr, and because they form deeply embedded in massive cloud cores, very little is known about the initial and environmental conditions of high-mass stellar birth. In general high-mass star forming regions are characterized by more extreme physical conditions than their low-mass counterparts, containing cores of size, mass, and velocity dispersion roughly an order of magnitude larger than those of cores in low-mass regions (e.g. Jijina et al. 1999; Garay & Lizano 1999; Kurtz et al. 2000; Beuther et al. 2007; Motte et al. 2008). Typical sizes of cluster-forming clumps are $\sim 1\,\mathrm{pc}$, they have mean densities of $n \sim 10^5\ \mathrm{cm}^{-3}$, masses of $\sim 10^3\,\mathrm{M}_\odot$ and above, and velocity dispersions ranging between 1.5 and $4\,\mathrm{km\,s}^{-1}$. Whenever observed with high resolution, these clumps break up in even denser cores, that are believed to be the immediate precursors of single or gravitationally bound multiple massive protostars.

Massive stars usually form as members of multiple stellar systems (Ho & Haschick 1981; Lada 2006; Zinnecker & Yorke 2007) which themselves are parts of larger clusters (Lada & Lada 2003; de Wit et al. 2004; Testi et al. 1997). This fact adds additional challenges to the interpretation of observational data from high-mass star forming regions as it is difficult to disentangle mutual dynamical interactions from the influence of individual stars (e.g. Goto et al. 2006; Linz et al. 2005). Furthermore, high-mass stars reach the main sequence while still accreting. Their Kelvin-Helmholtz pre-main sequence contraction time is considerably shorter than their accretion

thomas.peters@ita.uni-heidelberg.de
[1] Fellow of the Landesstiftung Baden-Württemberg
[2] Zentrum für Astronomie der Universität Heidelberg, Institut für Theoretische Astrophysik, Albert-Ueberle-Str. 2, D-69120 Heidelberg, Germany
[3] Kavli Institute for Particle Astrophysics and Cosmology, Stanford University, Menlo Park, CA 94025, U.S.A.
[4] Department of Astrophysics, American Museum of Natural History, 79th Street at Central Park West, New York, New York 10024-5192, USA

Work supported in part by US Department of Energy contract DE-AC02-76SF00515.

SLAC National Accelerator Laboratory, Menlo Park, CA 94025

time. Once a star has reached a mass of about $10\,M_\odot$ its spectrum becomes UV dominated and it begins to ionize its environment. This means that accretion as well as ionizing and non-ionizing radiation needs to be considered in concert (Keto 2002, 2003, 2007; Peters et al. 2010a). It has been realized decades ago that in simple 1-dimensional collapse models the outward radiation force on the accreting material should be significantly stronger than the inward pull of gravity (Larson & Starrfield 1971; Kahn 1974; Wolfire & Cassinelli 1987) in particular when taking dust opacities into account. Since stars as massive as $100-150\,M_\odot$ have been observed (Bonanos et al. 2004; Figer 2005; Rauw et al. 2005) a simple spherically symmetric approach to high-mass star formation is doomed to fail.

Consequently, two different models for massive star formation have been proposed. The first one takes advantage of the fact that high-mass stars always form as members of stellar clusters. If the central density in the cluster is high enough, there is a chance that low-mass protostars collide and so successively build up more massive objects (Bonnell et al. 1998). As the radii of protostars usually are considerably larger than the radii of main sequence stars in the same mass range this could be a viable option. However, the stellar densities required to produce very massive stars are still extremely high and seem inconsistent with the observed values of Galactic star clusters (e.g. Portegies Zwart et al. 2010, and references therein). An alternative approach is to argue that high-mass stars form just like low-mass stars by accretion of ambient gas that goes through a rotationally supported disk caused by angular momentum conservation. Indeed such disk structures are observed around a number of high-mass protostars (Chini et al. 2004, 2006; Jiang et al. 2008; Davies et al. 2010). Their presence breaks any spherical symmetry that might have been present in the initial cloud and thus solves the opacity problem. Radiation tends to break out along the polar axis, while matter is transported inwards through parts of the equitorial plane shielded by the disk. Hydrodynamic simulations in two and three dimensions using a flux-limited diffusion approach to the transport of non-ionizing radiation strongly support this picture (Yorke & Sonnhalter 2002; Krumholz et al. 2009). The same holds when focusing on the effects of ionizing radiation using ray-tracing methods (Peters et al. 2010a). If the disk becomes gravitationally unstable, material flows along dense, opaque filaments whereas the radiation escapes through optically thin channels in and above the disk. It has been demonstrated that even ionized material can be accreted, if the accretion flow is strong enough. H II regions are gravitationally trapped at that stage, but soon begin to rapidly fluctuate between trapped and extended states, in agreement with observations (Peters et al. 2010a; Galván-Madrid et al. 2010). Over time, the same ultracompact H II region can expand anisotropically, contract again, and take on any of the observed morphological classes (Wood & Churchwell 1989; Kurtz et al. 1994; Peters et al. 2010a,b). In their extended phases, expanding H II regions drive bipolar neutral outflows characteristic of high-mass star formation (Peters et al. 2010a).

Another key fact that any theory of massive star formation must account for is the apparent presence of an upper mass limit. No star more massive than $100-150\,M_\odot$ has been observed (Massey 2003). This holds for the Galactic field, however, it is also true for young star clusters that are massive enough so that purely random sampling of the initial mass function (IMF) (Kroupa 2002; Chabrier 2003) without upper mass limit should have yielded stars above $150\,M_\odot$ (Weidner & Kroupa 2004; Figer 2005; Oey & Clarke 2005; Weidner et al. 2010, see however, Selman & Melnick 2008). This immediately raises the question of what is the physical origin of this apparent mass limit. It has been speculated before that radiative stellar feedback might be responsible for this limit (see, e.g., Zinnecker & Yorke 2007) or alternatively that the internal stability limit of stars with non-zero metallicity lies in this mass regime (Appenzeller 1970b,a, 1987; Baraffe et al. 2001). However, fragmentation could also limit protostellar mass growth. Indeed, this is what we see in the simulations discussed here. The likelihood of fragmentation to occur and the number of fragments to form depends sensitively on the physical conditions in the star-forming cloud and its initial and environmental parameters (see, e.g., Girichidis et al. 2010). Understanding the build-up of massive stars, therefore, requires detailed knowledge about the physical processes that initiate and regulate the formation and dynamical evolution of the molecular clouds these stars form in (Vázquez-Semadeni et al. 2009).

We argue that ionizing radiation, just like its non-ionizing, lower-energy counterpart, cannot shut off the accretion flow onto massive stars. Instead it is the dynamical processes in the gravitationally unstable accretion flow that inevitably occurs during the collapse of high-mass cloud cores that control the mass growth of individual protostars. Accretion onto the central star is shut off by the fragmentation of the disk and the formation of lower-mass companions which intercept inward moving material. We call this process fragmentation-induced starvation and argue that it occurs unavoidably in regions of high-mass star formation where the mass flow onto the disk exceeds the inward transport of matter due to viscosity only and thus renders the disk unstable to fragmentation. We speculate that fragmentation-induced starvation is important not only for present-day star formation but also in the primordial universe during the formation of metal-free Population III stars. Consequently, we expect these stars to be in binary or small number multiple systems and to be of lower mass than usually inferred (Abel et al. 2002; Bromm et al. 2009). Indeed, current numerical simulations provide the first hints that this might be the case (Clark et al. 2008; Turk et al. 2009; Stacy et al. 2010).

In the current study, we analyze the simulations by Peters et al. (2010a) with special focus on the mass growth history of the individual stars forming and the physical processes that influence their accretion rate. We briefly review the numerical method we use and the assumptions and approximations behind it in Section 2. Then we describe our findings in Section 3 and discuss them in the context of present-day and primordial star formation in Section 4. We summarize and conclude in Section 5.

2. METHOD AND ASSUMPTIONS

We present three-dimensional, radiation-hydrodynamical simulations of massive star formation

that include heating by ionizing and non-ionizing radiation using the adaptive-mesh code FLASH (Fryxell et al. 2000). We use our improved version of the hybrid-characteristics raytracing method (Rijkhorst et al. 2006; Peters et al. 2010a) to propagate the radiation on the grid and couple sink particles (Federrath et al. 2010), which we use as models of protostars, to the radiation module via a prestellar model (Peters et al. 2010a).

The simulations start with a $1000\,M_\odot$ molecular cloud. The cloud has a constant density core of $\rho = 1.27\times10^{-20}$ $\mathrm{g\,cm^{-3}}$ within a radius of $r = 0.5\,\mathrm{pc}$ and then falls off as $r^{-3/2}$ until $r = 1.6\,\mathrm{pc}$. The initial temperature of the cloud is $T = 30\,\mathrm{K}$. The whole cloud is set up in solid body rotation with an angular velocity $\omega = 1.5\times10^{-14}\,\mathrm{s^{-1}}$ corresponding to a ratio of rotational to gravitational energy $\beta = 0.05$ and a mean specific angular momentum of $j = 1.27\times10^{23}\,\mathrm{cm^2 s^{-1}}$.

We follow the gravitational collapse of the molecular cloud with the adaptive mesh until we reach a cell size of 98 AU. We create sink particles at a cut-off density of $\rho_{\mathrm{crit}} = 7\times10^{-16}\,\mathrm{g\,cm^{-3}}$. All gas within the accretion radius of $r_{\mathrm{sink}} = 590\,\mathrm{AU}$ above ρ_{crit} is accreted to the sink particle if it is gravitationally bound to it. The Jeans mass on the highest refinement level is $M_{\mathrm{jeans}} = 0.13\,\mathrm{M_\odot}$.

The adaptive mesh technique allows us to resolve the gravitational collapse of the gas from the parsec scale down to a few hundred AU. At higher spatial resolution of only several ten AU, the gas becomes optically thick to non-ionizing radiation, and scattering effects must be taken into account. Since our cut-off density is more than two orders of magnitude smaller than the onset of the optically thick regime at $\sim10^{-13}\,\mathrm{g\,cm^{-3}}$ (e.g. Larson 1969) and we are focussing in our analysis on large-scale effects on the stellar cluster scale, we expect the raytracing approximation to be valid. Feedback by radiation pressure, which plays a role on the very small scales and is neglected in our model, is dynamically unimportant on these large scales (Krumholz & Matzner 2009).

We discuss three simulations (see Table 1). In the first simulation (run A), we only allow for the formation of a single sink particle and suppress the formation of secondary sink particles artificially by introducing the dynamical temperature floor

$$T_{\mathrm{min}} = \frac{G\mu}{\pi k_{\mathrm{B}}}\rho(n\Delta x)^2 \qquad (1)$$

with Newton's constant G, mean molecular weight μ, Boltzmann's constant k_{B}, local gas density ρ, and cell size Δx. The temperature floor ensures the sufficient resolution of the Jeans length with $n \geq 4$ cells, which avoids artificial fragmentation (Truelove et al. 1997). The suppression of secondary sink formation guarantees that the accretion flow around the massive star is not weakened by the fragmentation of the disk, which would otherwise inevitably lead to the formation of companion stars that limit the growth of the massive stars in the cluster (see Section 3). In the second simulation (run B), this dynamical temperature floor is not applied, and a whole stellar cluster forms during the simulation runtime. The third simulation (run D) is a control run that allows us to study the influence of radiation feedback on the stellar cluster evolution. As in run B, a small stellar cluster forms, but the stars emit no radiation, neither ionizing nor non-ionizing.

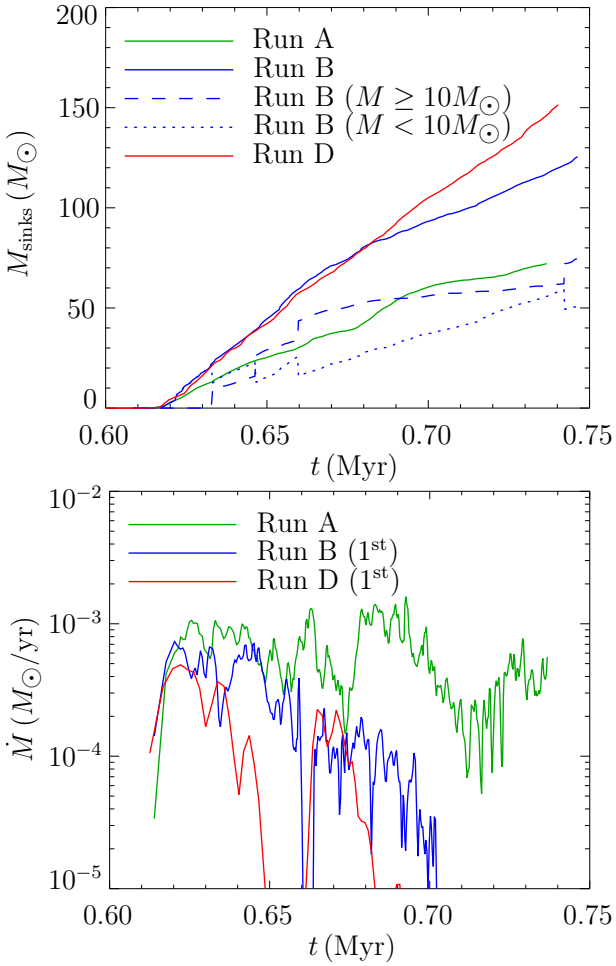

FIG. 1.— *top* Total accretion history of all sink particles combined forming in runs A, B, and D. While the heating by non-ionizing radiation does not affect the total star formation rate, the ionizing radiation appreciably reduces the total rate at which gas converts into stars once the most massive object has stopped accreting and its H II region can freely expand. This effect is not compensated by triggered star formation at the ionization front, which is never observed during the simulation runtime. The slope of the total accretion history in run B goes down because the massive stars (dashed line) accrete at a decreased rate, while the low-mass stars (dotted line) keep accreting at the same rate. *bottom* Instantaneous accretion rate as function of time of the first sink particle to form in the three runs. These are generally the most massive sink particles during most of the simulation runtime. While the accretion onto the star in run A never stops, the massive stars in run B and D are finally starved of material. Since the radiative heating suppresses fragmentation in run B, the final mass of the star is almost twice as high as in run D.

The numerical method along with its inherent physical limitations is discussed in detail in Peters et al. (2010a).

3. RESULTS

3.1. *Accretion History*

In this section we compare the protostellar mass growth rates from our three runs, with a single sink particle (run A), multiple sinks and radiative heating (run B), and multiple sinks with no radiative heating (run D) (see Section 2). As already discussed by Peters et al. (2010a), when only the central sink particle is allowed to form (run A), nothing stops the accretion flow to the center. Figure 1 shows that the central protostar

TABLE 1
Overview of collapse simulations.

Name	Resolution	Radiative Feedback	Multiple Sinks	$M_{\rm sinks}$ ($M_\odot$)	$N_{\rm sinks}$	$M_{\rm max}$ ($M_\odot$)
Run A	98 AU	yes	no	72.13	1	72.13
Run B	98 AU	yes	yes	125.56	25	23.39
Run D	98 AU	no	yes	151.43	37	14.64

Note. — We have run a simulation with a single sink particle (run A) to probe the upper mass limit with radiative feedback as well as simulations with multiple sink particles to study stellar cluster formation with (run B) and without (run D) radiative feedback. The simulations differ largely in the total mass in sink particles ($M_{\rm sinks}$), the total number of sink particles ($N_{\rm sinks}$) and the mass of the most massive star ($M_{\rm max}$) at the end of the simulation. We follow the notation introduced in Peters et al. (2010a), where additional low-resolution runs Ca und Cb were discussed.

grows at a rate $\dot{M} \approx 5.9 \times 10^{-4}\,{\rm M}_\odot\,{\rm yr}^{-1}$ until we stop the calculation when the star has reached $72\,{\rm M}_\odot$. The growing star ionizes the surrounding gas, raising it to high pressure. However this hot bubble soon breaks out above and below the disk plane, without affecting the gas flow in the disk[5] midplane much. In particular, it cannot halt the accretion onto the central star. Similar findings have also been reported from simulations focussing on the effects of non-ionizing radiation acting on somewhat smaller scales (Yorke & Sonnhalter 2002; Krumholz et al. 2007, 2009; Sigalotti et al. 2009). Radiation pressure is not able to stop accretion onto massive stars and is dynamically unimportant, except maybe in the centers of dense star clusters near the Galactic center (Krumholz & Matzner 2009).

The situation is different when the disk can fragment and form multiple sink particles. Initially the mass growth of the central protostar in runs B and D is comparable to the one in run A. However, as soon as further protostars form in the gravitationally unstable disk, they begin to compete with the central object for accretion of disk material. However, unlike in the classical competitive accretion picture (Bonnell et al. 2001a, 2004), it is not the most massive object that dominates and grows disproportionately fast. On the contrary, it is the successive formation of a number of low-mass objects in the disk at increasing radii that limits subsequent growth of the more massive objects in the inner disk. Material that moves inwards through the disk due to viscous and gravitational torques accretes preferentially onto the sinks at larger radii.

Similar behavior is found in models of low-mass protobinary disks, where again the secondary accretes at a higher rate than the primary. Its orbit around the common center of gravity scans larger radii and hence it encounters material that moves inwards through the disk before the primary star. This drives the system towards equal masses and circular orbits (Bate & Bonnell 1997; Bate 2000). In our simulations, after a certain transition period hardly any gas makes it all the way to the center and the accretion rate of the first sink particle drops to almost zero. This is the essence of the fragmentation-induced starvation process. In run B, it prevents any star from reaching a mass larger than $25\,{\rm M}_\odot$. The Jeans mass in run D is smaller than in run B because of the lack of accretion heating, and consequently the highest mass star in run D grows to less than $15\,{\rm M}_\odot$.

Inspection of Figure 1 reveals additional aspects of the process. We see that the total mass of the sink particle system increases at a faster rate in the multiple sink simulations, run B and D, than in the single sink case, run A. This is understandable, because as more and more gas falls onto the disk it becomes more and more unstable to fragmentation, so as time goes by additional sink particles form at larger and larger radii. Star formation occurs in a larger volume of the disk, and mass growth is not limited by the disk's ability to transport matter to its center by gravitational or viscous torques (compare Section 3.2). As a result the overall star-formation rate is larger than in run A.

Since the accretion heating raises the Jeans mass and length in run B, the total number of sink particles is higher in run D than in run B, and the stars in run D generally reach a lower mass than in run B (compare Section 4.2.2). These two effects cancel out to lead to the same overall star formation rate for some time. At one point in the evolution, however, also the total accretion rate of run B drops below that of run D. At time $t \approx 0.68\,{\rm Myr}$ the accretion flow around the most massive star has attenuated below the value required to trap the H II region. It is able to break out and affect a significant fraction of the disk area. A comparison with the mass growth of run D clearly shows that there is still enough gas available to continue constant cluster growth for another 50 kyr or longer, but the gas can no longer collapse in run B. Instead, it is swept up in a shell surrounding the expanding H II region. The figure furthermore demonstrates that, although the accretion rates of the most massive stars ($M \geq 10\,{\rm M}_\odot$) steadily decrease, the low-mass stars ($M < 10\,{\rm M}_\odot$), which do not produce any significant H II regions, keep accreting at the same rate.

It is also notable that the expanding ionization front around the most massive stars does not trigger any secondary star formation during the whole simulation runtime, which suggests that triggered star formation (Elmegreen & Lada 1977) may not be as efficient as expected, at least on the scales considered here.

Figure 2 shows the individual accretion histories of each of the sink particles in run B and run D. Radiative heating cannot prevent disk fragmentation but raises the local Jeans mass. Hence, as discussed above, much fewer stars form in run B than in run D, and the mass of the most massive stars in run B is higher. It is also evident from the figure that star formation is much more intermittent in the case with radiation feedback (run B). The reason for this behavior is that the star formation process is controlled by the local Jeans mass, which depends to a large degree on how the filaments in the disk shield the radiation (compare Section 3.2). Shielding can lower the Jeans mass temporarily and thereby allow gravitational collapse that would not have occured otherwise.

[5] We will hereafter refer to the flattened, dense, accretion flow that forms in the midplane of our rotating core as a disk. However, it is not necessarily a true Keplerian, viscous, accretion disk, which probably only forms within the central few hundred astronomical units, unresolved by our models.

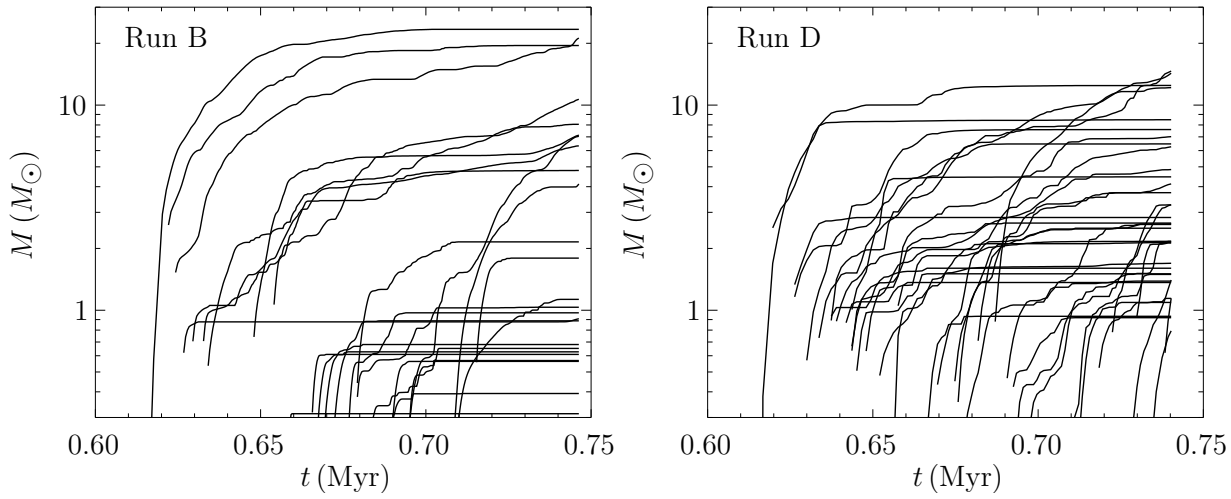

FIG. 2.— Individual accretion histories for run B and run D. The figure shows the stellar masses as function of time for all sink particles that form in run B (*left*) and run D (*right*). Because the Jeans mass is lower without radiative feedback (run D), many more sink particles form in run D than in run B, and the mass of the most massive stars is also lower.

The accretion histories also reveal large differences between sink particles within the same simulation. For example, in run D a sink particle that forms around $t \approx 0.688\,\mathrm{Myr}$ accretes very rapidly and becomes one of the most massive stars in the cluster while other stars only accrete sporadically, interrupted with long intervals of no accretion at all, and some others even accrete only shortly after their formation. There are several reasons for these differences. First, accretion can stop when stars are ejected from the cluster by N-body interactions. This happens mostly to low-mass stars with masses $M \lesssim 2\mathrm{M}_\odot$. Second, intermediate-mass stars can be starved of material by the formation of companions. This is the essential element of the fragmentation-induced starvation scenario. A star that can grow to intermediate masses is embedded in an accretion flow with a larger gas reservoir. If this reservoir is gravitationally unstable, it can collapse to form companions. This may explain why the intermediate-mass stars in run B seem to have shorter time intervals of no accretion. Since the Jeans mass is higher in this case, the formation of companions is suppressed, and this allows the star to accrete for longer times. Third, the stars are not fixed at a position in the disk plane but move quickly within the disk by gravitational interaction with their surrounding dense gas and with nearby stars. Hence, they are not tied to the filament they form in but can move away from it. If the star moves into a low-density void in the disk, accretion will stop until the star is embedded in higher density gas again. The sink particle in run D mentioned above accretes so vigorously because it moves along with its parental filament over a long time and no companions form around it. Fourth, accretion can stop when the star resides within a low-density H II region. This applies to the first two massive stars in run B. Their accretion flow had become so weak that the ionizing radiation was able to isolate the stars from the high-density gas in the disk and stopped accretion.

3.2. *Disk Growth and Disk Instability*

To quantify the accretion of mass onto the disk and the subsequent instability, we calculate the amount of mass in a control volume that encloses the disk at all times. This control volume is the same for all runs and has dimensions $0.24\,\mathrm{pc}\times0.24\,\mathrm{pc}\times0.015\,\mathrm{pc}$. We show in Figure 3 the mass M_disk of non-accreted gas contained in the control volume, the mass M_sinks contained in all sink particles as well as the total mass $M_\mathrm{tot} = M_\mathrm{disk} + M_\mathrm{sinks}$ for runs A, B and D. The disk mass in run A is much larger than in the multiple sink runs B and D since the mass cannot be absorbed by secondary sink particles. Instead, the mass accumulates in the disk plane. Consequently, the star in run A is embedded in a strong accretion flow at all times, which facilitates accretion at an approximately constant rate despite radiation feedback. The evolution in runs B and D differs from the mass growth in run A as soon as secondary sink particles form. The continuous formation of new sink particles in these runs keeps M_disk almost constant. At $t \approx 0.64\,\mathrm{Myr}$, strong ionization-driven outflows (see Peters et al. 2010a) begin to reduce M_disk in run B, so that it falls below the case without feedback (run D) at late times. The accretion onto sink particles, however, is not affected by this and stays at a constant rate until the H II region can break free as discussed above (compare Figure 1).

We investigate the initial instability of the disk with an analysis of the Toomre Q-parameter

$$Q = \left|\frac{2c_\mathrm{s}\Omega}{\pi\Sigma G}\right|$$

with sound speed c_s, angular velocity Ω, surface density Σ, and Newton's constant G. The disk is linearly stable for $Q > 1$ and linearly unstable for $Q < 1$ (Toomre 1964; Goldreich & Lynden-Bell 1965). The initial phases of disk instability in run B are displayed in Figure 4. The figure shows slices of density, temperature and Q in the disk plane for four different times. One can clearly see that the most unstable parts of the disk are the filamentary structures that form as the disk grows in mass. The heating by stellar radiation can suppress instability locally, but shielding by the dense filaments prevents the whole disk from becoming stable and restricts the heating to small regions near the center of the disk that are surrounded by filaments. This shielding makes it possible for star formation to progress radially outwards despite accretion heating by the stars. The disk remains suffi-

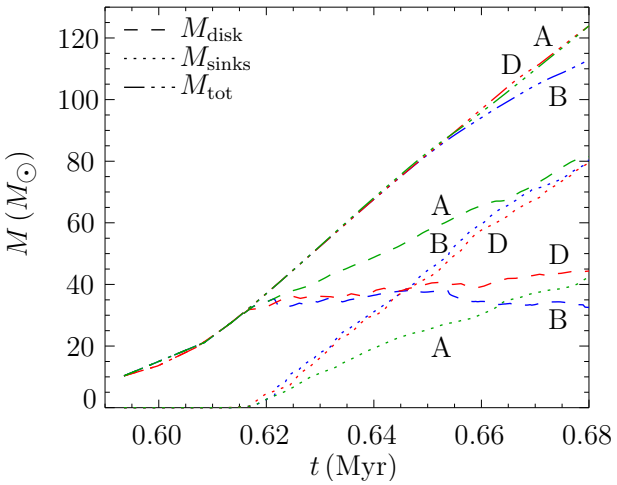

FIG. 3.— Disk growth and sink particle formation. The plot shows the mass $M_{\rm disk}$ of non-accreted gas contained in a control volume around the disk, the mass $M_{\rm sinks}$ of all sink particles and the total mass $M_{\rm tot} = M_{\rm disk} + M_{\rm sinks}$ for run A (green), run B (blue) and run D (red). The disk mass in runs B and D is kept almost constant by subsequent sink particle formation, while the disk in run A continuously grows. The deviation between the disk masses in runs B and D at late times is caused by ionization-driven outflows, but these do not affect the total star formation rate.

ciently cool at the inner edge for gravitational instability to set in and star formation proceeds inside-out in the disk plane. Hence, the effect of the filamentary structures in the disk is twofold: they are so dense that they render the disk unstable locally; and, because of their high density, they can effectively shield the radiation from the stellar cluster near the center of the disk, so that radiative heating does not stabilize the outer parts of the disk. Indeed, high-resolution observations of high-mass accretion disk candidates (Beuther et al. 2009) provide some evidence for fragmentation and the presence of substructure on $\sim 1000\,{\rm AU}$ scales.

To illustrate the tendency of star formation to occur at increasingly larger disk radii, we show the disk radius at which new sink particles form as a function of time for runs B and D in Figure 5. Because the accretion heating sets in already with the very first stars that form in run B, sink formation is suppressed at small disk radii initially. The massive stars slowly spiral outwards with time, so that at $t \approx 0.67\,{\rm Myr}$ their radiation can be shielded by filaments in the disk. Within these filaments, the gas then cools until local collapse sets in and two sink particles form near the center of the disk. Once the filament has dissolved, the gas heats up again and no further sink particles form in the inner disk region.

4. DISCUSSION

4.1. *Initial Conditions*

4.1.1. *Density Profile*

As we argue above, the fragmentation behavior of the disk forming around the massive central star depends sensitively on the initial and boundary conditions, i. e. on the physical properties of the high-mass cloud core. One of the key parameters that determines whether fragmentation becomes widespread during the collapse of a massive cloud core is its initial density profile. Numerical simulations indicate that density profiles with flat inner core are strongly susceptible to fragmentation, while centrally concentrated cores (for example such as singular isothermal spheres with $\rho \propto r^{-2}$) usually form only one or at most a few objects (Girichidis et al. 2010).

The density structure of prestellar cores is typically estimated through the analysis of dust emission or absorption using near-IR extinction mapping of background starlight, mapping of millimeter/submillimeter dust continuum emission, and mapping of dust absorption against the bright mid-IR background emission (Bergin & Tafalla 2007). A main characteristic of the density profiles derived with the above techniques is that they require a central flattening. The density of low-mass cores is almost constant within radii smaller than $2500 - 5000\,{\rm AU}$ with typical central densities of 10^5 – 10^6 cm^{-3} (Motte et al. 1998; Ward-Thompson et al. 1999). A popular approach is to describe these cores as truncated isothermal (Bonnor-Ebert) sphere (Ebert 1955; Bonnor 1956), that often provides a good fit to the data (Bacmann et al. 2001; Alves et al. 2001; Kandori et al. 2005). Bonnor-Ebert spheres are equilibrium solutions of self-gravitating gas bounded by external pressure. However, such density structure is not unique. Numerical calculations of the dynamical evolution of supersonically turbulent clouds show that transient cores forming at the stagnation points of convergent flows exhibit similar morphology (Ballesteros-Paredes et al. 2003; Banerjee et al. 2009). The situation is less clear when it comes to high-mass cores (Beuther et al. 2007), because most high-mass cores studied to date show at least some sign of star formation or turn out to consist of several subcondensations when observed with high enough resolution (e.g. Beuther et al. 2005; Beuther & Henning 2009). However, large-scale surveys, e.g. as conducted in the Cygnus-X region (Motte et al. 2007), indicate that high-mass cores are in many aspects similar to scaled-up versions of low-mass cores. We followed these lines of reasoning and chose an initial density profile with flat inner core and $r^{-1.5}$ density profile outside a radius of $r = 0.5\,{\rm pc}$.

4.1.2. *Rotation*

The second important parameter is the initial rotation of this core, which defines the total amount of angular momentum in the system and hence the radial extent of the protostellar accretion disk. To assess the relevance of fragmentation-induced starvation for high-mass star formation we therefore must compare our choice of $\beta = 0.05$ for the ratio between rotational and potential energy in our $1000\,M_\odot$ core both with observational data of molecular cloud cores and with numerical simulations of core formation. Our choice of values correspond to a specific angular momentum of $j = 1.27 \times 10^{23}\,{\rm cm^2 s^{-1}}$.

The high-mass cloud cores observed by Pirogov et al. (2003) with masses up to a few thousand solar masses show specific angular momenta j from a few $\times 10^{22}\,{\rm cm^2 s^{-1}}$ up to $10^{23}\,{\rm cm^2 s^{-1}}$, corresponding to β-values up to 0.07. We took this sample as motivation for our choice of parameters. Interesting in this context is also the large-scale rotational motion of molecular gas around a cluster of hypercompact H II regions in G20.08-0.14 N seen by Galván-Madrid et al. (2009). This flow has a radius of about 0.5 pc, roughly consistent with our simulation. Similar observations were made by Keto (1990) for G10.6-0.4 and Welch et al. (1987) for W94A.

It needs to be noted, however, that although the spe-

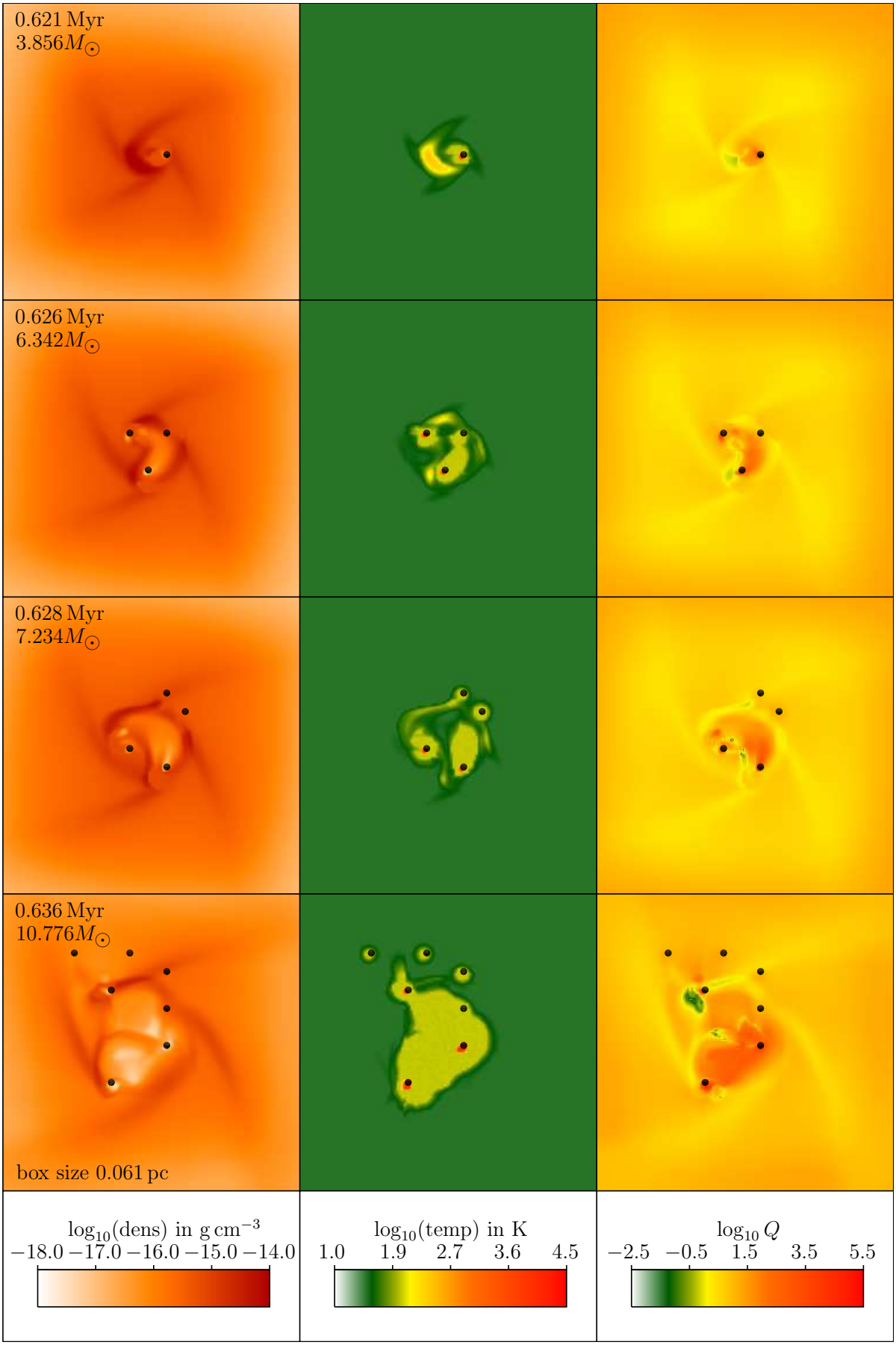

FIG. 4.— Early phase of disk instability in run B. The panels show slices of density, temperature and the Toomre Q-parameter at four different times. Each frame shows the simulation runtime and the mass of the most massive star in the cluster. The black dots indicate the positions of sink particles. One can see how the stellar radiation initially heats up the disk locally, which enhances the stability. The dense filaments, however, shield the radiation, and the cold material within and behind the filaments becomes unstable again.

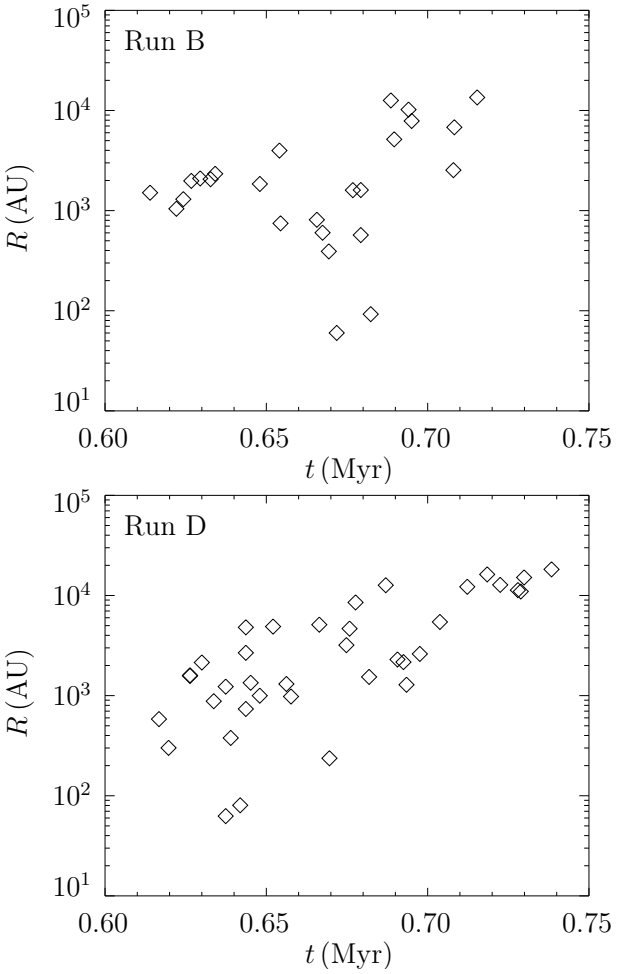

FIG. 5.— Radius of sink formation as a function of time for run B (*top*) and run D (*bottom*). Because of the absence of radiation heating, both the Jeans length and the Jeans mass are smaller in run D than in run B, giving rise to the formation of more numerous, but generally lower-mass stars. In both simulations, sink formation gradually occurs at larger disk radii. The accretion heating by the first stars to form suppresses sink formation at small disk radii in run B until relatively late in the cluster evolution.

cific angular momenta of observed cores exhibit considerable scatter there is a clear trend of decreasing j with decreasing core mass M. For example, the mean values in the sample discussed by Goodman et al. (1993) are $j \approx 6 \times 10^{21}\,\mathrm{cm^2 s^{-1}}$ with masses up to several hundred solar masses, while Caselli et al. (2002) studied low-mass cores with typically only a few solar masses and find $j \approx 7 \times 10^{20}\,\mathrm{cm^2 s^{-1}}$. In all cases the typical values for the ratio between rotational energy and potential energy is $\beta \lesssim 0.05$. This trend continues down to stellar scales. A binary G star with a orbital period of 3 days has $j \approx 10^{19}\,\mathrm{cm^2\,s^{-1}}$, while the spin of a typical T Tauri star is a few $\times 10^{17}\,\mathrm{cm^2\,s^{-1}}$. Our own Sun rotates only with $j \approx 10^{15}\,\mathrm{cm^2\,s^{-1}}$. That means, during the process of star formation most of the initial angular momentum is removed from the collapsed object (Bodenheimer 1995).

If we look for guidance from numerical simulations of molecular cloud formation and fragmentation (Mac Low & Klessen 2004; Klessen et al. 2009) we see a very similar trend. Gammie et al. (2003) find a typical mean specific angular momentum of $j = 4 \times 10^{22}\,\mathrm{cm^2 s^{-1}}$, while Jappsen & Klessen (2004) find values in the range $10^{20}\,\mathrm{cm^2 s^{-1}} \lesssim j \lesssim 10^{21}\,\mathrm{cm^2 s^{-1}}$ for low-mass cores in the simulations by Klessen et al. (1998) and Klessen & Burkert (2001, 2000) depending on the evolutionary state of protostellar collapse. See also Tilley & Pudritz (2007) and Offner et al. (2008). Altogether, we find that our initial conditions are consistent with simulations of core formation.

4.2. *Relation to Other Theoretical Models*

4.2.1. *Monolithic Collapse Models*

The monolithic collapse model rests on the similarity between the shape of the observed core mass distribution (Motte et al. 1998; Johnstone et al. 2000, 2006; Lada et al. 2008) and the stellar initial mass function, IMF (Kroupa 2002; Chabrier 2003). It assumes a one-to-one relation between the distributions with only a constant efficiency factor separating the two functions. Each molecular cloud core collapses to form a single star or at most a close binary system, with protostellar feedback processes determining the efficiency of the process (Matzner & McKee 2000). This model reduces the problem of the origin of the IMF to the problem of determining the mass spectrum of bound cores, although strictly speaking the idea that the IMF is set by the mass spectrum of cores is independent of any particular model for the origin of that mass spectrum. Arguments to explain the core mass distribution generally rely on the statistical properties of turbulence (Klessen 2001; Padoan & Nordlund 2002; Hennebelle & Chabrier 2008, 2009), which generate structures with a pure powerlaw mass spectrum. The thermal Jeans mass in the cloud then imposes the flattening and turn-down in the observed mass spectrum.

However, there are a number of caveats. Many of the prestellar cores found in observational surveys appear to be stable entities and thus are unlikely to be in a state of active star formation. In addition, the simple interpretation that one core forms on average one star, and that all cores contain the same number of thermal Jeans masses, leads to a timescale problem (Clark et al. 2007) that requires differences in the core mass function and the IMF. Other concern about this model comes from hydrodynamic simulations, which seem to indicate that massive cores should fragment into many stars rather than collapsing monolithically (Dobbs et al. 2005; Clark & Bonnell 2006; Bonnell & Bate 2006; Federrath et al. 2010). This objection is, however, weakened by the fact that magnetic fields are able to reduce the level of fragmentation on scales of molecular clouds as a whole (Heitsch et al. 2001) as well as of collapsing cloud cores (Hennebelle & Fromang 2008; Hennebelle & Teyssier 2008). In addition, radiative feedback also is able to reduce the number of fragments that form during the collapse of high-mass cores (Krumholz et al. 2007). But again, all current simulations indicate that neither accretion heating nor ionizing radiation can prevent the fragmentation of the massive dense disk that builds up during protostellar collapse, nor can they stop accretion onto the massive star (Yorke & Sonnhalter 2002; Krumholz et al. 2009; Peters et al. 2010a). Instead, the heating merely increases the average mass of the fragments. This is also supported by analytic estimates comparing typical accretion rates onto the disk with its ability to transport matter inwards through viscous and gravitational torques (Krat-

ter & Matzner 2006; Kratter et al. 2010). Our current results agree with these studies.

4.2.2. *Competitive Accretion*

A second model for the origin of the IMF, called competitive accretion, focuses on the interaction between protostars, and between a protostellar population and the gas cloud around it (Bonnell et al. 2001a,b; Bonnell & Bate 2002; Bate & Bonnell 2005). In the competitive accretion picture the origin of the peak in the IMF is similar to the monolithic collapse model, it is set by the Jeans mass in the prestellar gas cloud. However, rather than fragmentation in the gas phase producing a spectrum of core masses, each of which collapses down to a single star or star system, in the competitive accretion model all gas fragments down to roughly the Jeans mass. Prompt fragmentation therefore creates a mass function that lacks the powerlaw tail at high masses that we observe in the stellar mass function. This part of the distribution forms via a second phase in which Jeans mass-protostars compete for gas in the center of a dense cluster. The cluster potential channels mass towards the center, so stars that remain in the center grow to large masses, while those that are ejected from the cluster center by N-body interactions remain low mass (Klessen & Burkert 2000; Bonnell et al. 2004). In this model, the apparent similarity between the core and stellar mass functions is an illusion, because the observed cores do not correspond to gravitationally bound structures that will collapse to stars (Clark & Bonnell 2006; Smith et al. 2008).

The competitive accretion picture has been challenged, on the grounds that the kinematic structure observed in star-forming regions is inconsistent with the idea that protostars have time to interact with one another strongly before they completely accrete their parent cores (Krumholz et al. 2005; André et al. 2007).

Taken at face value, competitive accretion models show a correlation between the mass of the most massive star $M_{\rm max}$ and the total cluster mass $M_{\rm sinks}$ during the whole cluster evolution that is roughly $M_{\rm max} \propto M_{\rm sinks}^{2/3}$ (Bonnell et al. 2004). This correlation has been argued to represent a way to observationally confirm competitive accretion (Krumholz & Bonnell 2007) and is in fact in good agreement with observations (Weidner & Kroupa 2006; Weidner et al. 2010). However, we find that our simulations also reproduce the observed relation between $M_{\rm max}$ and $M_{\rm sinks}$.

Figure 6 shows $M_{\rm sinks}$ as function of $M_{\rm max}$ for run A, run B and run D along with the relation $M_{\rm max} = 0.39 M_{\rm sinks}^{2/3}$, which was found by Bonnell et al. (2004) as a fit to their simulation data. Over the whole cluster evolution, the curve for run D lies above this fit, while the curve for run B always lies below it. The fit agrees with our simulation data as well as it does to that of Bonnell et al. (2004). This indicates that the scaling is not unique to competitive accretion, but can also be found with the fragmentation-induced starvation scenario and hence cannot be used as an observational confirmation of competitive accretion models.

The agreement of both models to this prediction is surprising because the accretion behavior of the most massive stars is totally different. Whereas the massive stars in competitive accretion simulations automatically accrete large fractions of the available gas because they reside in the center of the gravitational potential during the whole cluster evolution, the massive stars in fragmentation-induced starvation models have continuously decreasing accretion rates since they are starved of material by other cluster members and, in the final phase, by feedback from ionizing radiation. It seems that the observed relation between $M_{\rm sinks}$ and $M_{\rm max}$ is a very general result of protostellar interaction in a common cluster environment, and not an unambiguous sign of competitive accretion at work.

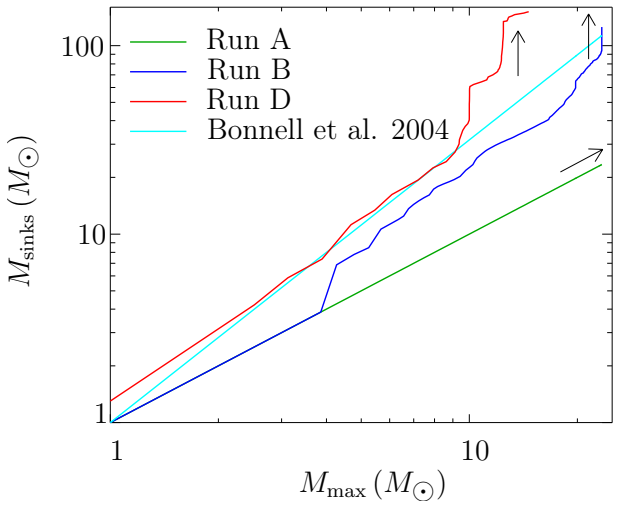

FIG. 6.— The total mass in sink particles $M_{\rm sinks}$ as function of the most massive star in the cluster $M_{\rm max}$. We plot the curves for run A, run B and run D as well as the fit from the competitive accretion simulations Bonnell et al. (2004). Both simulations follow the competitive accretion prediction with good accuracy. The maximum mass $M_{\rm max}$ in run B is always larger than in run D for a fixed cluster mass $M_{\rm sinks}$. The turn-off away from the scaling relation (indicated by arrows) is shifted towards higher masses by radiative feedback.

We can gain further insight from Figure 6. It shows that the accretion heating suppresses low-mass star formation and that for all times the simulation with feedback contains a more massive star relative to the whole cluster mass than the simulation without feedback. When the most massive star in run D reaches $10\,{\rm M}_\odot$, much more gas is used up to create additional low-mass stars than is funneled towards the most massive one. Thus, the growth of the most massive star in run D is much more ineffective than in run B. Remarkably, all four simulations in Bonnell et al. (2004) show the turn-off towards accretion onto low-mass stars around $10\,{\rm M}_\odot$, and only one simulation has formed a star more massive than $10\,{\rm M}_\odot$. A very similar turn-off (indicated by an arrow in Figure 6) at the same mass scale is found in run D, but the radiative heating in run B shifts the turn-off towards higher masses, so that the scaling is followed closely over a larger mass range. In fact, since the turn-off occurs only at the end of the simulation and some of the massive stars are still accreting at this point, it is unknown up to what mass the scaling will continue. However, these results clearly indicate that radiative feedback is necessary to reproduce the scaling for masses beyond $10\,{\rm M}_\odot$ observed by Weidner et al. (2010).

4.3. *Relevance for Primordial Star Formation*

We note that the initial conditions adopted here may also be appropriate for the formation of metal-free Population III stars. The very first generation of stars in the universe is thought to form at a redshift of $z \sim 15$ in relatively unperturbed and quiescent halos with masses of $\sim 10^6\,\mathrm{M}_\odot$ in dark matter and about $10^5\,\mathrm{M}_\odot$ in baryons (Bromm & Larson 2004; Bromm et al. 2009). This gas has primordial composition, i.e. basically consists of hydrogen and helium, and cools mostly via H_2 line emission (e.g. Anninos et al. 1997; Glover 2005; Glover & Jappsen 2007). These halos have a well-defined density structure and rotational profile (Abel et al. 2002) which leads to the build up of an extended accretion disk around the central object (see, e.g., Yoshida et al. 2008 for numerical simulations, or Tan & McKee 2004 for an analytical model). Just as discussed above, if the mass flow onto the disk exceeds its capacity for transporting material inward by viscous torques, the disk becomes susceptible to gravitational instability and fragments. There are first indications that this indeed happened during Pop III star formation from high-resolution numerical simulations that follow gravitational collapse beyond the formation of the central hydrostatic protostar (Clark et al. 2008; Turk et al. 2009; Stacy et al. 2010). We propose that fragmentation-induced starvation may be the physical process that determines the masses of Pop III stars.

The situation is very different in atomic cooling halos (Wise & Abel 2007; Greif et al. 2009). Once the virial mass of a halo exceeds a value of $\sim 10^8\,\mathrm{M}_\odot$, the infalling gas gets partially ionized in the virialization shock. The enhanced abundance of free electrons triggers rapid H_2 formation and some fraction of the gas cools down very rapidly. As a result there are streams of cold gas that can travel all the way to the center (see also Dekel et al. 2009) and the overall velocity structure of the gas becomes highly chaotic and turbulent. We expect that these environmental conditions prevent the build-up of a large-scale accretion disk in the center of the halo and our model of fragmentation-induced starvation should therefore not be applicable. However, a more thorough analysis awaits the execution of detailed, high-resolution numerical simulations.

5. SUMMARY AND CONCLUSION

We have presented a detailed analysis of the fragmentation-induced starvation scenario, which was first introduced by Peters et al. (2010a). We have studied the accretion history and disk instability in collapse simulations of massive star formation. We have compared the results from a full simulation with radiation feedback and multiple sink particles with two control runs, one with multiple sink particles but without radiation feedback and one with radiation feedback but only a single sink particle. The combined analysis of all three simulations allows us to establish fragmentation-induced starvation as a workable model of massive star formation. We have also compared the new model to the monolithic collapse and competitive accretion models and speculated on the relevance of fragmentation-induced starvation for primordial star formation.

The basic principle of fragmentation-induced starvation is star formation in a rotating gravitationally unstable flow. Gravitational instability in such a flow leads to fragmentation of the accretion flow and the formation of companions around the central massive star that starve the central star of infalling material. In our simulations, star formation occurs within a rotationally flattened, disk-like structure. As more and more material falls onto the disk, star formation proceeds radially outwards, keeping the total disk mass roughly constant. The accretion history of individual stars is tightly connected with the position of these stars relative to the dense filaments and low-density voids in the disk. The fact that most if not all high-mass stars are observed in higher-order multiple stellar systems that themselves belong to more massive star clusters provides strong evidence for the widespread occurrence of fragmentation that forms the basis of our discussion.

We find that accretion heating does not prevent fragmentation of the disk, but leads to a higher local Jeans mass. As a result, fewer stars form with than without radiation feedback. The accretion heating shifts the masses of the most massive stars up, but leaves the average stellar mass almost unaffected. The accretion heating does not change the overall star formation rate of the whole stellar cluster. Feedback by ionizing radiation is unable to stop protostellar growth if the accretion flow is strong enough. However, if the accretion flow weakens due to starvation, an H II region can expand and terminate the accretion process. The growing H II regions reduce the total star formation rate and do not trigger star formation at the ionization front.

Our model is able to explain the observed morphologies (Peters et al. 2010b) and time variability (Galván-Madrid et al. 2010) of ultracompact H II regions. We find that we can consistently reproduce the observed relation between the total mass of the star cluster M_{sinks} and the maximum stellar mass in the cluster M_{max}, $M_{\mathrm{max}} \propto M_{\mathrm{sinks}}^{2/3}$. This relation seems to be the general outcome of protostellar interaction in a common cluster environment rather than being a signpost of competitive accretion only, as previously claimed. In fact, the dynamical processes discussed here exhibit exactly the opposite behavior of competitive accretion, rather than run-away accretion onto the most massive star together with the suppression of the growth of lower-mass objects, we see that angular momentum conservation and the presence of lower-mass objects limit the mass growth of massive stars.

Our simulations provide evidence for the rejection of proposals that the observed maximum stellar mass of $\sim 100\,\mathrm{M}_\odot$ is set by radiative feedback. When disk fragmentation is artificially suppressed (run A) the central protostar accretes material at very high rate unimpeded by the intense UV radiation it emits without any indications of an upper limit (see also Peters et al. 2010a). When we permit disk fragmentation to occur, it is the process of fragmentation-induced starvation that prevents the stellar mass to become larger than $\sim 25\,\mathrm{M}_\odot$ with our choice of initial conditions. We expect more massive, more centrally-condensed, and/or slower rotating cloud cores to lead to more massive protostars. This, however, needs to be confirmed in future studies. The alternative view is to attribute the apparent stellar mass limit to internal stability constraints.

T.P. is a Fellow of the *Landesstiftung Baden-*

Württemberg funded by their program International Collaboration II (grant P-LS-SPII/18). He also acknowledges support from an Annette Kade Fellowship for his visit to the American Museum of Natural History and a Visiting Scientist Award of the Smithsonian Astrophysical Observatory (SAO). R.S.K. acknowledges financial support from the *Landesstiftung Baden-Württemberg* via their program International Collaboration II (grant P-LS-SPII/18) and from the German *Bundesministerium für Bildung und Forschung* via the ASTRONET project STAR FORMAT (grant 05A09VHA). R.S.K. furthermore gives thanks for subsidies from the *Deutsche Forschungsgemeinschaft* (DFG) under grants no. KL 1358/1, KL 1358/4, KL 1359/5, KL 1358/10, and KL 1358/11, as well as from a Frontier grant of Heidelberg University sponsored by the German Excellence Initiative. R.S.K. also thanks the KIPAC at Stanford University and the Department of Astronomy and Astrophysics at the University of California at Santa Cruz for their warm hospitality during a sabbatical stay in spring 2010. M.-M.M.L. was partly supported by NSF grant AST 08-35734. R.B. is funded by the DFG via the Emmy-Noether grant BA 3607/1-1. We acknowledge computing time at the Leibniz-Rechenzentrum in Garching (Germany), the NSF-supported Texas Advanced Computing Center (USA), and at Jülich Supercomputing Centre (Germany). The FLASH code was in part developed by the DOE-supported Alliances Center for Astrophysical Thermonuclear Flashes (ASCI) at the University of Chicago.

REFERENCES

Abel, T., Bryan, G. L., & Norman, M. L. 2002, Science, 295, 93
Alves, J. F., Lada, C. J., & Lada, E. A. 2001, Nature, 409, 159
André, P., Belloche, A., Motte, F., & Peretto, N. 2007, A&A, 472, 519
Anninos, P., Zhang, Y., Abel, T., & Norman, M. L. 1997, New Astron., 2, 209
Appenzeller, I. 1970a, A&A, 9, 216
—. 1970b, A&A, 5, 355
Appenzeller, I. 1987, in Astrophysics and Space Science Library, Vol. 136, Instabilities in Luminous Early Type Stars, ed. H. J. G. L. M. Lamers & C. W. H. de Loore, 55–67
Bacmann, A., André, P., & Ward-Thompson, D. 2001, in Astronomical Society of the Pacific Conference Series, Vol. 243, From Darkness to Light: Origin and Evolution of Young Stellar Clusters, ed. T. Montmerle & P. André, 113–124
Ballesteros-Paredes, J., Klessen, R. S., & Vázquez-Semadeni, E. 2003, ApJ, 592, 188
Banerjee, R., Vázquez-Semadeni, E., Hennebelle, P., & Klessen, R. S. 2009, MNRAS, 398, 1082
Baraffe, I., Heger, A., & Woosley, S. E. 2001, ApJ, 550, 890
Bate, M. R. 2000, MNRAS, 314, 33
Bate, M. R. & Bonnell, I. A. 1997, MNRAS, 285, 33
—. 2005, MNRAS, 356, 1201
Bergin, E. A. & Tafalla, M. 2007, ARA&A, 45, 339
Beuther, H., Churchwell, E. B., McKee, C. F., & Tan, J. C. 2007, in Protostars and Planets V, ed. B. Reipurth, D. Jewitt, & K. Keil (The University of Arizona Press), 165–180
Beuther, H. & Henning, T. 2009, A&A, 503, 859
Beuther, H., Sridharan, T. K., & Saito, M. 2005, ApJ, 634, L185
Beuther, H., Walsh, A. J., & Longmore, S. N. 2009, ApJS, 184, 366
Bodenheimer, P. 1995, ARA&A, 33, 199
Bonanos, A. Z., Stanek, K. Z., Udalski, A., Wyrzykowski, L., Żebruń, K., Kubiak, M., Szymański, M. K., Szewczyk, O., Pietrzyński, G., & Soszyński, I. 2004, ApJ, 611, L33
Bonnell, I. A. & Bate, M. R. 2002, MNRAS, 336, 659
—. 2006, MNRAS, 370, 488
Bonnell, I. A., Bate, M. R., Clarke, C. J., & Pringle, J. E. 2001a, MNRAS, 323, 785
Bonnell, I. A., Bate, M. R., & Zinnecker, H. 1998, MNRAS, 298, 93
Bonnell, I. A., Clarke, C. J., Bate, M. R., & Pringle, J. E. 2001b, MNRAS, 324, 573
Bonnell, I. A., Vine, S. G., & Bate, M. R. 2004, MNRAS, 349, 735
Bonnor, W. B. 1956, MNRAS, 116, 351
Bromm, V. & Larson, R. B. 2004, ARA&A, 42, 79
Bromm, V., Yoshida, N., Hernquist, L., & McKee, C. F. 2009, Nature, 459, 49
Caselli, P., Benson, P. J., Myers, P. C., & Tafalla, M. 2002, ApJ, 572, 238
Chabrier, G. 2003, PASP, 115, 763
Chini, R., Hoffmeister, V., Kimeswenger, S., Nielbock, M., Nürnberger, D., Schmidtobreick, L., & Sterzik, M. 2004, Nature, 429, 155
Chini, R., Hoffmeister, V. H., Nielbock, M., Scheyda, C. M., Steinacker, J., Siebenmorgen, R., & Nürnberger, D. 2006, ApJ, 645, L61
Clark, P. C. & Bonnell, I. A. 2006, MNRAS, 368, 1787
Clark, P. C., Glover, S. C. O., & Klessen, R. S. 2008, ApJ, 672, 757
Clark, P. C., Klessen, R. S., & Bonnell, I. A. 2007, MNRAS, 379, 57
Davies, B., Lumsden, S. L., Hoare, M. G., Oudmaijer, R. D., & de Wit, W.-J. 2010, MNRAS, 402, 1504
de Wit, W. J., Testi, L., Palla, F., Vanzi, L., & Zinnecker, H. 2004, A&A, 425, 937
Dekel, A., Birnboim, Y., Engel, G., Freundlich, J., Goerdt, T., Mumcuoglu, M., Neistein, E., Pichon, C., Teyssier, R., & Zinger, E. 2009, Nature, 457, 451
Dobbs, C. L., Bonnell, I. A., & Clark, P. C. 2005, MNRAS, 360, 2
Ebert, R. 1955, Z. Astrophys., 37, 217
Elmegreen, B. G. & Lada, C. J. 1977, ApJ, 214, 725
Federrath, C., Banerjee, R., Clark, P. C., & Klessen, R. S. 2010, ApJ, 713, 269
Figer, D. F. 2005, Nature, 434, 192
Fryxell, B., Olson, K., Ricker, P., Timmes, F. X., Zingale, M., Lamb, D. Q., MacNeice, P., Rosner, R., Truran, J. W., & Tufo, H. 2000, ApJS, 131, 273
Galván-Madrid, R., Keto, E., Zhang, Q., Kurtz, S., Rodríguez, L. F., & Ho, P. T. P. 2009, ApJ, 706, 1036
Galván-Madrid et al. 2010, in preparation
Gammie, C. F., Lin, Y.-T., Stone, J. M., & Ostriker, E. C. 2003, ApJ, 592, 203
Garay, G. & Lizano, S. 1999, PASP, 111, 1049
Girichidis et al. 2010, in preparation
Glover, S. 2005, Space Sci. Rev., 117, 445
Glover, S. C. O. & Jappsen, A.-K. 2007, ApJ, 666, 1
Goldreich, P. & Lynden-Bell, D. 1965, MNRAS, 130, 97
Goodman, A. A., Benson, P. J., Fuller, G. A., & Myers, P. C. 1993, ApJ, 406, 528
Goto, M., Stecklum, B., Linz, H., Feldt, M., Henning, T., Pascucci, I., & Usuda, T. 2006, ApJ, 649, 299
Greif, T. H., Johnson, J. L., Klessen, R. S., & Bromm, V. 2009, MNRAS, 399, 639
Heitsch, F., Mac Low, M.-M., & Klessen, R. S. 2001, ApJ, 547, 280
Hennebelle, P. & Chabrier, G. 2008, ApJ, 684, 395
—. 2009, ApJ, 702, 1428
Hennebelle, P. & Fromang, S. 2008, A&A, 477, 9
Hennebelle, P. & Teyssier, R. 2008, A&A, 477, 25
Ho, P. T. P. & Haschick, A. D. 1981, ApJ, 248, 622
Jappsen, A.-K. & Klessen, R. S. 2004, A&A, 423, 1
Jiang, Z., Tamura, M., Hoare, M. G., Yao, Y., Ishii, M., Fang, M., & Yang, J. 2008, ApJ, 673, L175
Jijina, J., Myers, P. C., & Adams, F. C. 1999, ApJS, 125, 161
Johnstone, D., Matthews, H., & Mitchell, G. F. 2006, ApJ, 639, 259
Johnstone, D., Wilson, C. D., Moriarty-Schieven, G., Joncas, G., Smith, G., Gregersen, E., & Fich, M. 2000, ApJ, 545, 327
Kahn, F. D. 1974, A&A, 37, 149

Kandori, R., Nakajima, Y., Tamura, M., Tatematsu, K., Aikawa, Y., Naoi, T., Sugitani, K., Nakaya, H., Nagayama, T., Nagata, T., Kurita, M., Kato, D., Nagashima, C., & Sato, S. 2005, AJ, 130, 2166
Keto, E. 2002, ApJ, 580, 980
—. 2003, ApJ, 599, 1196
—. 2007, ApJ, 666, 976
Keto, E. R. 1990, ApJ, 355, 190
Klessen, R. S. 2001, ApJ, 556, 837
Klessen, R. S. & Burkert, A. 2000, ApJS, 128, 287
—. 2001, ApJ, 549, 386
Klessen, R. S., Burkert, A., & Bate, M. R. 1998, ApJ, 501, L205
Klessen, R. S., Krumholz, M. R., & Heitsch, F. 2009, arxiv: 0906.4452v1
Kratter, K. M. & Matzner, C. D. 2006, MNRAS, 373, 1563
Kratter, K. M., Matzner, C. D., Krumholz, M. R., & Klein, R. I. 2010, ApJ, 708, 1585
Kroupa, P. 2002, Science, 295, 82
Krumholz, M. R. & Bonnell, I. A. 2007, arxiv:0712.0828v2
Krumholz, M. R., Klein, R. I., & McKee, C. F. 2007, ApJ, 656, 959
Krumholz, M. R., Klein, R. I., McKee, C. F., Offner, S. S. R., & Cunningham, A. J. 2009, Science, 323, 754
Krumholz, M. R. & Matzner, C. D. 2009, ApJ, 703, 1352
Krumholz, M. R., McKee, C. F., & Klein, R. I. 2005, Nature, 438, 332
Kurtz, S., Cesaroni, R., Churchwell, E., Hofner, P., & Walmsley, C. M. 2000, in Protostars and Planets IV, ed. V. Mannings, A. P. Boss, & S. S. Russell (The University of Arizona Press), 299–326
Kurtz, S., Churchwell, E., & Wood, D. O. S. 1994, ApJS, 91, 659
Lada, C. J. 2006, ApJ, 640, L63
Lada, C. J. & Lada, E. A. 2003, ARA&A, 41, 57
Lada, C. J., Muench, A. A., Rathborne, J., Alves, J. F., & Lombardi, M. 2008, ApJ, 672, 410
Larson, R. B. 1969, MNRAS, 145, 271
Larson, R. B. & Starrfield, S. 1971, A&A, 13, 190
Linz, H., Stecklum, B., Henning, T., Hofner, P., & Brandl, B. 2005, A&A, 429, 903
Mac Low, M.-M. & Klessen, R. S. 2004, Rev. Mod. Phys., 76, 125
Massey, P. 2003, ARA&A, 41, 15
Matzner, C. D. & McKee, C. F. 2000, ApJ, 545, 364
McKee, C. F. & Ostriker, E. C. 2007, ARA&A, 45, 565
Motte, F., André, P., & Neri, R. 1998, A&A, 336, 150
Motte, F., Bontemps, S., Schilke, P., Schneider, N., Menten, K. M., & Broguière, D. 2007, A&A, 476, 1243
Motte, F., Bontemps, S., Schneider, N., Schilke, P., & Menten, K. M. 2008, in Astronomical Society of the Pacific Conference Series, Vol. 387, Massive Star Formation: Observations Confront Theory, ed. H. Beuther, H. Linz, & T. Henning, 22–29
Oey, M. S. & Clarke, C. J. 2005, ApJ, 620, L43
Offner, S. S. R., Klein, R. I., & McKee, C. F. 2008, ApJ, 686, 1174
Padoan, P. & Nordlund, Å. 2002, ApJ, 576, 870
Peters, T., Banerjee, R., Klessen, R. S., Mac Low, M.-M., Galván-Madrid, R., & Keto, E. R. 2010a, ApJ, 711, 1017
Peters, T., Mac Low, M.-M., Banerjee, R., Klessen, R. S., & Dullemond, C. P. 2010b, ArXiv e-prints
Pirogov, L., Zinchenko, I., Caselli, P., Johansson, L. E. B., & Myers, P. C. 2003, A&A, 405, 639
Portegies Zwart, S. F., McMillan, S. L. W., & Gieles, M. 2010, ARA&A, 48, in press
Rauw, G., Crowther, P. A., De Becker, M., Gosset, E., Nazé, Y., Sana, H., van der Hucht, K. A., Vreux, J.-M., & Williams, P. M. 2005, A&A, 432, 985
Rijkhorst, E.-J., Plewa, T., Dubey, A., & Mellema, G. 2006, A&A, 452, 907
Selman, F. J. & Melnick, J. 2008, ApJ, 689, 816
Sigalotti, L. D. G., de Felice, F., & Daza-Montero, J. 2009, ApJ, 707, 1438
Smith, R. J., Clark, P. C., & Bonnell, I. A. 2008, MNRAS, 391, 1091
Stacy, A., Greif, T. H., & Bromm, V. 2010, MNRAS, 403, 45
Tan, J. C. & McKee, C. F. 2004, ApJ, 603, 383
Testi, L., Palla, F., Prusti, T., Natta, A., & Maltagliati, S. 1997, A&A, 320, 159
Tilley, D. A. & Pudritz, R. E. 2007, MNRAS, 382, 73
Toomre, A. 1964, ApJ, 139, 1217
Truelove, J. K., Klein, R. I., McKee, C. F., Hollman II, J. H., Howell, L. H., & Greenough, J. A. 1997, ApJ, 489, L179
Turk, M. J., Abel, T., & O'Shea, B. 2009, Science, 325, 601
Vázquez-Semadeni, E., Gómez, G. C., Jappsen, A.-K., Ballesteros-Paredes, J., & Klessen, R. S. 2009, ApJ, 707, 1023
Ward-Thompson, D., Motte, F., & André, P. 1999, MNRAS, 305, 143
Weidner, C. & Kroupa, P. 2004, MNRAS, 348, 187
—. 2006, MNRAS, 365, 1333
Weidner, C., Kroupa, P., & Bonnell, I. A. D. 2010, MNRAS, 401, 275
Welch, W. J., Dreher, J. W., Jackson, J. M., Terebey, S., & Vogel, S. N. 1987, Science, 238, 1550
Wise, J. H. & Abel, T. 2007, ApJ, 665, 899
Wolfire, M. G. & Cassinelli, J. P. 1987, ApJ, 319, 850
Wood, D. O. S. & Churchwell, E. 1989, ApJS, 69, 831
Yorke, H. W. & Sonnhalter, C. 2002, ApJ, 569, 846
Yoshida, N., Omukai, K., & Hernquist, L. 2008, Science, 321, 669
Zinnecker, H. & Yorke, H. W. 2007, ARA&A, 45, 481